https://doi.org/10.18321/ectj1327

Hydrocarbon Synthesis from CO_2 and H_2 Using the Ultrafine Iron-Containing Catalytic Systems Based on Carbonized Cellulose

M.V. Kulikova*, M.V. Chudakova, M.I. Ivantsov, O.S. Dementyva, A.L. Maksimov

A.V. Topchiev Institute of Petrochemical Synthesis, RAS, 29 Leninsky ave., Moscow, Russia

Article info

Received:
10 April 2022

Received in revised form:
24 May 2022

Accepted:
26 June 2022

Keywords:
Hydrothermal carbonization, Carbon carrier, CO_2 hydrogenation, Product distribution

Abstract

Carbon materials were formed by the hydrothermal carbonization of cellulose, which were used as support for carbon dioxide hydrogenation catalysts (Fe/C and Fe-Mn/C). In the presence of these catalytic systems, CO_2 conversion reached 50%. It is shown that the manganese introduction into the Fe-containing catalytic system significantly affects the distribution of gaseous C_1-C_4 products and liquid C_{5+} hydrocarbons. Promotion leads to the suppression of methane formation and an increase in the proportion of C_2-C_4 light olefins in gaseous products, as well as to intensification of secondary processes with the formation of a significant amount of iso-structures in liquid products. The different distribution of C_1-C_6 alcohols in the oxygen-containing products on the Fe/C and Fe-Mn/C catalysts indicates the manganese effect on the routes of their formation.

1. Introduction

Carbon dioxide (CO_2) is one of the most important sources of climate change. The greenhouse effect is known to be associated with an increase in the content of carbon dioxide [1]. Currently, various ways to reduce greenhouse gas emissions into the atmosphere are being considered. To limit CO_2 emissions into the atmosphere and restore the natural balance, the following decision is proposed [2]: removal CO_2 from the total emission balance. This can be achieved through the organization of geological gas storages or its chemical processing with the high value-added product production. Both of these methods require the creation of efficient technologies, the development of which has been actively underway since the early 2000s. However, the issue of involving CO_2 in reactions that are traditionally carried out with the use of carbon monoxide arose at the dawn of the synthetic hydrocarbon production era. Therefore, in [3] the formation of methane from mixtures containing carbon monoxide and carbon dioxide on various nickel catalysts was discussed. Back in the 1930s, the authors of these works set the goal of determining whether the fact that carbon dioxide slows down the hydrogenation reaction of CO is a general pattern. Later in [4] it has been suggested that the formation of carbon monoxide is an intermediate step in the synthesis of higher hydrocarbons. And already in 1936 it was proved that the synthesis of hydrocarbons from CO_2 and H_2 goes through the stage of carbon monoxide formation [5] according to the scheme:

$$CO \rightarrow CO \rightarrow CH_2 \rightarrow (CH_2)_n.$$

According to many contemporary authors [6], the hydrogenation of CO_2 to liquid hydrocarbons usually occurs using a bifunctional water shift reaction catalyst to form CO and subsequent hydrogenation of CO to hydrocarbons (Fischer-Tropsch synthesis). Based on this postulate, it is obvious that the approaches of highly efficient Fischer-Tropsch catalysts development should also be relevant for catalytic systems used for carbon dioxide hydrogenation.

*Corresponding author.
E-mail addresses: m_kulikova@ips.ac.ru

Recently, fibrous carbon materials have been increasingly used as carriers for the active component of heterogeneous catalysts for the Fischer-Tropsch synthesis. For example, the use of a carbon nanofiber with homogeneously dispersed iron nanoparticles (promoted with sulfur and sodium) makes it possible to form an effective catalyst for the hydrogenation of CO to light olefins (selectivity for C_2-C_4 olefins up to 60 wt.%) [7].

Currently, metal-carbon catalysts compete with traditional oxide-supported catalysts due to their stability in acidic and alkaline media. Activated carbons, carbon black, graphite and graphitized materials are commonly used as carbon carriers [8]. For example, in the synthesis by the organic matric method the properties of the obtained materials are largely determined by the initial polymer choice and the conditions for its carbonization [9, 10].

Hydrothermal carbonization (HTC) is a modern method for obtaining carbon material (biochar) from various types of biomass. [11]. Compared to traditional thermal processing methods, HTC proceeds under mild conditions (process temperature up to 230 °C, pressure up to 30 atm). The surface of the material formed is saturated with C-H-O reactive centers (for example, hydroxyl, carbonyl, carboxyl functional groups) capable of interacting with the active phase of the catalyst [12]. Carbon materials obtained by HTC find applications in various fields, and can also be used as catalyst carriers for different processes [13]. The authors [14] formed a highly active catalyst for the carbon dioxide methane conversion, which consisted of molybdenum carbide nanoparticles (6–20 nm) deposited on biochar produced HTC. In [15] Pd catalysts supported by HTC obtained carbon microspheres for the efficient formic acid oxidation was developed. The method of furfural and palladium salt low-temperature hydrothermal synthesis makes it possible to form catalysts containing Pd nanoparticles on the surface of hydrophilic carbon spheres, which showed high activity in the hydrogenation of phenol (or its derivatives) to cyclohexanone (or its derivatives) [16]. The FTIR spectroscopy was applied to establish that introduction of aluminum at the stage of HTC cellulose leads to the surface aluminum-containing crystalline structure formation. These structures contribute to cellulose hydrolysis with the formation of an additional amount of oxygen-containing functional groups on the biochar surface, which promote the isomerization of glucose to fructose [17].

Catalysts based on carbon materials obtained by the HTC of biomass were studied under the conditions of the Fischer-Tropsch synthesis in some works. In [18] biochar obtained from wood (pine) was used as a carrier. The resulting iron-containing catalytic systems of the «core-shell» type showed high activity under the conditions of the Fischer-Tropsch synthesis. The CO conversion was 95% with a selectivity to liquid hydrocarbons of 68%, while high olefin content was observed in the products [19]. Spherical iron-carbon-containing catalytic systems were formed by glucose and iron nitrate HTC synthesis. It was found that the resulting carbonaceous material promotes the Hägg carbide creation, which ensures the formation of C_{5+} hydrocarbons under the conditions of the Fischer-Tropsch synthesis. In particular, the hydrothermal carbonization of cellulose makes it possible to influence the structure of the resulting carbon spheres and control their size, surface, and the presence of functional groups [20]. In [21] activated carbonized material was used as the CO_2 adsorbent and showed uptake of 84.5 mg CO_2 g^{-1}.

A set of physicochemical properties makes carbon materials obtained by the HTC method extremely promising for use as carriers for catalysts, [22], including their application for hydrogenation of CO and CO_2.

The hydrogenation of carbon monoxide to a mixture of hydrocarbons is a Fischer–Tropsch synthesis, an industrial process, [23], while the use of carbon dioxide as a feedstock is of great interest since CO_2 emissions are one of the main sources of climate change.

Since, according to scheme, the hydrogenation of carbon dioxide includes a reverse water shift reaction and the hydrogenation of the formed carbon monoxide [24], iron-containing catalysts are most suitable due to their ability to catalyze both reactions. In addition, iron-containing catalysts for the Fischer-Tropsch synthesis have some advantages (availability and low cost, ability to operate at a high CO/H_2 = 1–2 ratio, great technological flexibility, i.e. the possibility of synthesizing compounds of various groups), which makes it possible to use them for a wide range of product production [25]. Another distinguishing feature of iron catalysts is their stability Alkali metal carbonates, copper and manganese are most often used as energy promoters for iron catalysts (regardless of their method of preparation) [26, 27].

This study aimed to investigate the activity of catalytic systems Fe-/Fe-Mn – carbon, obtained

from carbonized cellulose, in the reaction of CO_2 hydrogenation.

2. Experimental

2.1. Catalyst preparation

Cellulose was used as s raw material (CAS 9004-34-6, China). To carry out the process of hydrothermal carbonization, a steel autoclave reactor with a volume of 0.5 L was used. Raw material (cellulose) with weight m feed = 50 g was mixed with water in a ratio 1/4 and then placed into the reactor. The reactor was heated to 190 °C and maintained in isothermal mode for 24 h. Then the reactor was cooled, and the resulting suspension was filtered on filter paper (filter paper pore size 3–5 μm). The solid residue (carbonizate) was dried at 105 °C for 24 h. The resulting carbonizate m feed = 8.5 g with weight was thermally treated in an inert atmosphere in a muffle furnace at 400 °C for 1 h. The heat treatment temperature was determined from a thermogravimetric study. The resulting stabilized carbonizate m feed = 4.799 g was impregnated with a joint solution of metal nitrates with 6.5 g of iron nitrate ($Fe(NO_3)_3 \cdot 9H_2O$, «extra pure», manufacturer Scharlau Chemie S.A), 1.57 g of manganese nitrate ($Mn(NO_3)_2 \cdot 6H_2O$, «extra Pure», manufactured by Junsei Chemicals) and 0.047 g of potassium nitrate (KNO_3, «extra pure», manufactured by ChemElements) dissolved in 8.2 ml of a water-alcohol solution (1:1 vol.) and dried in a water bath. After complete drying, the sample was thermally treated in an inert atmosphere in a muffle furnace at 400 °C for 1 h.

2.2. Characterization of catalysts

X-ray phase analysis was carried out on a Rigaku Rotaflex D/MAX-RC X-ray diffractometer (Rigaku, Japan). A rotating copper anode and a secondary graphite monochromator (CuKα radiation wavelength 0.1542 nm) were used as an X-ray source in the continuous θ-2θ scanning mode in the angular range 2θ = 10÷100º, scanning speed 2°/min, scanning step 0, 04°. The experimental diffraction patterns were processed using the MDI Jade 6.5 program; the phase composition was identified using the ICDD PDF-2 diffraction database. The quantitative composition was evaluated using the MDI Jade 6.5 program using the Reference Intensity Ratio method (RIR) which does not require the preparation of samples with an internal [28].

The thermo-programmed reduction (TPR) was conducted during linear heating with fixation of the hydrogen uptake process was carried out in a flow quartz reactor (diameter 2 mm) with temperature control by a thermocouple at atmospheric pressure in the temperature range from room temperature to 800 °C. The H_2/Ar gas flow (hydrogen content, 5% vol.) and the hydrogen content in the outgoing gas flow were determined on a katharometer using a Kristallux-4000 M (Meta-Khrom, Russia) chromatograph. The weighed portion of the catalyst ranged from 30 to 50 mg, depending on the content of the metal component.

2.3. Catalytic activity tests

Catalytic investigations were carried out in a fixed bed reactor. Before the catalytic tests, samples were reduced by H_2 at 450 °C and 20 bar pressure with 1000 h^{-1} GHSV for 3 h. Synthesis was conducted in a continuous mode at 20 bar pressure and reacting gas (mixture of CO_2 and H_2 with molar ratio CO_2:H_2 = 1:3) 500 h^{-1} GHSV in the temperature range from 240 to 320 °C. The temperature was increased stepwise (by 20 °C every 12 h). Gas and liquid products were analyzed at the end of each isothermal run.

The reacting gas and gaseous products were analyzed on a Kristallux-4000 M chromatograph (Meta-Khrom, Russia) with two chromatographic columns – CaA molecular sieve packed column (3 mm × 3 m) under an isothermal temperature regime (80 °C) and A Haye Sep R packed column (3 m × 3 mm) under the programmable regime (80–200 °C, 8 °C min^{-1}). Helium was used as a carrier gas, and a thermal conductivity detector was used as a detector.

Liquid hydrocarbons were analyzed by gas-liquid chromatography (GLC) on a Kristallux-4000 M chromatograph equipped with a flame ionization detector. A 50 m × 0.32 mm capillary column filled with OV-351 was used. Temperature-program mode: 50 °C (2 min); 50–260 °C, 6 °C/min; 260–270 °C, 5 °C/min; 270 °C (10 min).

Oxygenates in the aqueous phase were analyzed by GLC on a Kristallux-4000 M chromatograph equipped with a flame ionization detector. A 50 m × 0.32 mm capillary column packed with HP-FFAP (nitroterephthalic modified polyethylene glycol) was used. Temperature-program mode: 70 °C (8 min); 70–110 °C, 10 °C/min; 110–220 °C, 15 °C/min; 220 °C (10 min). Isobutyl alcohol was used as an internal standard.

The activity of the catalyst was estimated according to the following indicators: X_{CO_2}, % – CO_2 conversion (percentage of reacted carbon dioxide mass to CO_2 supplied mass to reaction zone), product yield (product grams quantity obtained by passing 1 m^3 of reacting gas through the catalyst).

3. Results and discussion

The introduction of a promoting additive (Mn) into the catalyst composition has little effect on the activity in the synthesis of hydrocarbons from CO_2 and H_2 (Table 1). In the presence of the formed Fe/C and Fe-Mn/C catalysts, with an increase in the synthesis temperature, the CO_2 conversion smoothly increases from 28 to 48%, and the maximum conversion degree (48%) is reached at a temperature of 320 °C.

It can be seen (Table 1) that in the case of an unpromoted catalyst, the activity reaches a plateau in the range of 280–320 °C, and in the presence of a Fe-Mn/C catalyst, the maximum of C_{5+} hydrocarbons are formed at a temperature of 280 °C. Thus, it is impractical to carry out hydrogenation of carbon dioxide at temperatures above 320 °C.

It is important to note that with a comparable activity of the Fe/C and Fe-Mn/C catalytic systems in the carbon dioxide hydrogenation, the distribution of gaseous and liquid products differs significantly. In the presence of Fe/C, the methane content in the gas phase increases with synthesis temperature rise and reaches 24 g/m^3 at 320 °C, whereas with the introduction of manganese into the catalyst, the methane yield does not exceed 13 g/m^3 over the entire temperature range. In addition, paraffin predominates in the gaseous C_2-C_4 products obtained in the presence of Fe/C: the yield of n-C_2-C_4 is 14 g/m^3, and the yield of C_2-C_4 olefins is 4 g/m^3, and the promotion of the catalyst leads to an increase in the yield of olefins to 12 g/m^3 with a simultaneous decrease in the yield of n-C_2-C_4 to 4 g/m^3.

Such a change in the distribution of gaseous reaction products – the suppression of methane formation and an increase in the proportion of light C_2-C_4 olefins – was recorded under the conditions of the Fischer-Tropsch synthesis and is explained by the influence of manganese, which is an energy promoter of iron-containing catalysts [29, 30, 31]. The authors [31] explain the increase in olefin selectivity by the fact that the introduction of magnesium reduces the hydrogenating function of the catalyst due to a decrease in H_2 adsorption and an increase in CO adsorption. In addition, the suppression of the formation of methane is associated with a more intense course of dissociative adsorption of CO on the surface of the promoted catalyst.

An increase in the CO content in the composition of the products was observed, which indicates the water gas reaction intensification to the formation of products. In the presence of the Fe/C catalytic system, the carbon monoxide yield practically did not increase with a synthesis temperature increase, which indicates that the catalyst does not intensify the water gas reverse reaction. The liquid C_{5+} hydrocarbon yield on a monometallic iron catalyst changed insignificantly with increasing temperature and amounted to 19.4–22 g/m^3. The promotion of the sample with manganese contributed to an increase in the yield of C_{5+} liquid hydrocarbons, and the maximum yield reached 34.8 g/m^3 at 300 °C (Table 1).

Table 1

The main indicators of CO_2 hydrogenation in the presence of catalysts based on carbonized cellulose

Sample	T, °C	X_{CO_2}, %	Yield, g/m^3					
			B_{CH4}	B_{C2-C4}	$B_{=C2-C4}$	B_{C5+}	B_{oxy}	B_{CO}
Fe/C	240	27.8	11.5	5.5	0.5	19.4	2.8	6.8
	260	32.0	13.8	9.3	0.7	19.1	3.4	7.3
	280	39.0	17.5	13.8	1.5	21.2	2.1	8.2
	300	44.9	21.5	15.2	3.0	2.21	4.5	8.4
	320	46.7	24.0	14.5	4.1	22.3	2.4	10.7
Fe-Mn/C	240	28.1	6.5	5.3	1.8	20.5	1.6	16.3
	260	34.8	5.4	1.8	7.6	29.7	2.6	14.5
	280	42.1	7.6	2.2	10.1	34.7	5.1	13.5
	300	46.9	10.1	2.8	12.2	34.8	8.2	14.3
	320	48.2	12.9	3.6	12.5	32.6	6.5	17.7

Table 2
Group and fractional composition of liquid products of hydrocarbon synthesis from CO_2 and H_2 in the presence of the systems under study at 320 °C

	Group composition, %			Fractional composition, %		
	n-paraffins	iso-paraffins	olefins	C_5-C_{10}	C_{11}-C_{18}	C_{19+}
Fe/C	55.6	21.1	20.3	35.9	58.2	5.9
Fe-Mn/C	20.0	49.9	30.1	52.0	41.5	6.5

In this case, the composition of C_{5+} hydrocarbons largely depends on the composition of the catalyst (Table 2).

On the monometallic catalyst, liquid hydrocarbons predominantly consist of C_{11}-C_{18} paraffin. The promotion of the catalyst with manganese leads to the formation of lighter hydrocarbons (C_5-C_{10}), while the content of iso-structures reaches 50%. Based on that the liquid hydrocarbon production in the CO_2 hydrogenation proceeds through the stage of CO production, then such an amount of iso-paraffins in the liquid products is most likely formed by secondary isomerization reactions [32]. The increase of the paraffin content from 20 to 30% in the liquid products with the introduction of manganese is in good agreement with the distribution of paraffin and olefins for gaseous C_2-C_4 products C_2-C_4.

An interesting feature of the studied catalysts is the C_1-C_6 alcohol distribution in the reaction products (Table 3).

At low synthesis temperatures (240–280 °C), methanol predominated in the alcohol fraction obtained on the Fe/C sample (50–39 wt.%, respectively), and its content decreased with increasing temperature due to more intense ethanol formation. In the products obtained on the Fe-Mn/C catalyst, the main component of the alcohol phase is ethanol. This difference indicates different routes for the formation of C_2-C_6 alcohols.

Figure 1 shows the Anderson-Schulz-Flory (ASF) distribution for alcohols produced on Fe/C and Fe-Mn/C catalysts. It can be seen that in the case of the monometallic catalyst, there is practically no deviation from the linear dependence (Fig. 1 (a)), while for the catalyst promoted with manganese, there is a clear exclusion of the first homologue from the distribution (Fig. 1 (b)). Such an effect was recorded in the presence of catalysts based on carbonized cellulose obtained by the organic matrix method under the conditions of carbon monoxide hydrogenation [10].

Most likely, in the presence of the Fe/C catalyst, oxymethylene radicals are formed on the catalyst surface and alcohols are formed through their polycondensation (Fig. 1 (a)), which is in good agreement with the distribution of oxygen-containing products. In the composition of alcohols obtained on Fe-Mn/C, there is practically no methanol in the entire temperature range (Table 3), and the ethanol content reached 80% at a temperature of 300 °C. This indicates that C_{2+}OH alcohols are formed by the methanol homologation reaction. A similar effect was also found in the study of the synthesis of alcohols from CO and H_2 in the presence of iron-sibunit catalysts [33].

In the presence of these catalysts, it is possible to obtain alcohols with a yield of 86 g/m^3, in which the C_2-C_4 content reaches 81–82%. This is once again indirect evidence that in catalytic systems of the metal-carbon type, the production of hydrocarbons and oxygenates flows through the stage of CO production.

To determine the effect of manganese on the properties of the obtained catalysts and their catalytic activity, Fe/C and Fe-Mn/C were studied by XRD and TPR methods (Figs. 2 and 3).

Table 3
Alcohols composition dependence of obtained on studied catalysts under the temperature of carbon dioxide hydrogenation process

Sample	Synthesis temperature, °C	Alcohol content, %mass					
		C_1	C_2	C_3	C_4	C_5	C_6
Fe/C	240	50	40	6	2	1	1
	260	50	41	6	2	1	1
	280	39	50	6	3	1	1
	300	34	53	7	3	2	1
	320	31	54	9	4	1	1
Fe-Mn/C	240	17	62	10	6	3	1
	260	5	68	12	7	5	3
	280	1	69	11	8	8	3
	300	1	80	11	5	3	1
	320	1	73	14	7	4	1

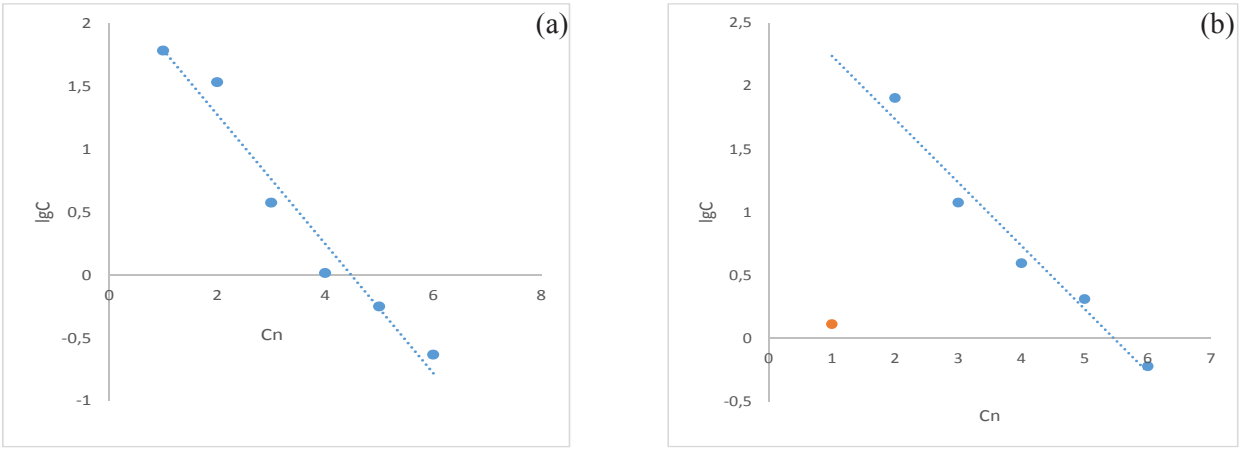

Fig. 1. Typical alcohols distribution (ASF) in logC-Cn coordinates for Fe/C (a) and Fe-Mn/C (b).

The Fe/C sample before catalytic tests is practically amorphous, the X-ray pattern contains significantly broadened reflections that belong to the magnetite phase (Fig. 2(1)).

When the catalytic system was reduced with hydrogen at 450 °C, according to the TPR profile of the Fe/C (Fig. 2 (1)), the formation of a magnetite phase occurred. Since the curve has a broad Fe_2O_3 reduction peak at 420 °C with a shoulder at 540 °C, which indicates the formation of a magnetite phase and its further reduction to FeO or a mixture of FeO-Fe°. The formation of magnetite at the activation stage initiates a reverse water-gas shift reaction with the CO formation [34].

During the Fischer-Tropsch synthesis, the magnetite phase (2θ = 30.08; 35.43; 43.05; 56.94; 62.52° (JCPDS-79-0419) and Hägg carbide

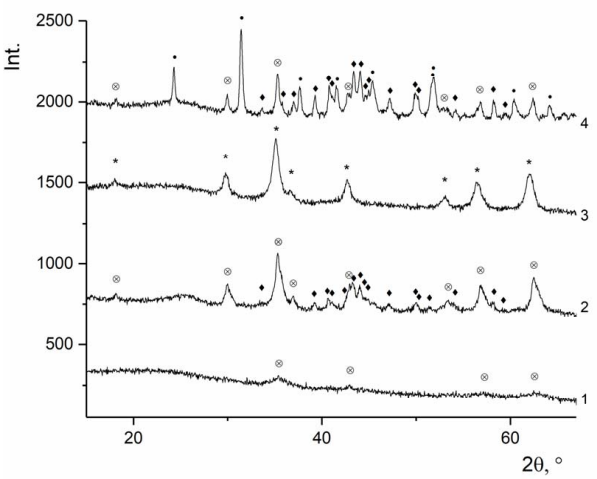

Fig. 2. X-ray patterns of Fe/C and Fe-Mn/C catalyst samples: 1 – catalyst Fe/C before catalytic tests; 2 – catalyst Fe/C after catalytic tests; 3 – catalyst Fe-Mn/C before catalytic tests; 4 – catalyst Fe-Mn/C after catalytic tests (• – reflexes $MnCO_3$; ♦ – χ-Fe_5C_2; * – $Mn_{0.43}Fe_{2.57}O_4$; ⊗ – Fe_3O_4).

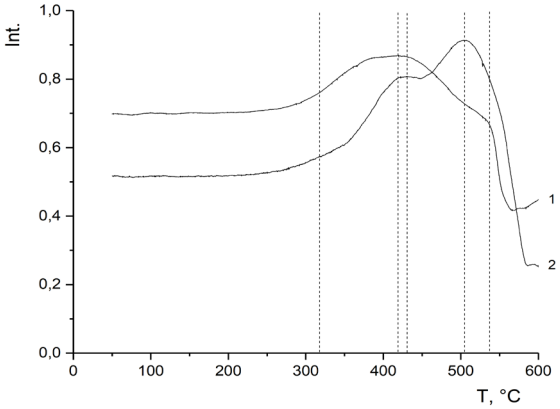

Fig. 3. TPR-profile of catalytic systems: 1 – Fe/C; 2 – Fe-Mn/C. I. $Fe_2O_3 \rightarrow Fe_3O_4 \rightarrow Fe°$. II. $Fe_2O_3 \rightarrow Fe_3O_4 \rightarrow FeO \rightarrow Fe°$.

(2θ = 39.31; 40.83; 41.15; 43.40; 44.07; 47.18° (JCPDS-51-0997)) is formed (Fig. 2 (2)). A polymerization process occurs on Hägg carbide with the formation of C_{5+} hydrocarbons [35]. The sizes of crystallites determined by the Debye-Scherrer method were: Fe_3O_4 – 10 nm, χ-Fe_5C_2 – 20 nm.

The initial Fe-Mn/C catalyst sample (Fig. 2 (3)) is ferromanganese oxide nanoparticles (JCPDS-89-2807) with a crystallite size of about 14 nm. An undivided peak appeared in the reduction profile of the Fe-Mn/C sample at a temperature of about 330 °C (Fig. 3 (2)), which is typical for Mn systems [36, 37, 38]: at this temperature, the Mn^{3+} phase is formed [37].

The peak at 430° is associated with the MnO formation, while the peak at 505° can be attributed to the reduction of the iron-containing phase to Fe_3O_4, since Fe-Mn systems are characterized by a shift in the reduction of Fe_2O_3 to higher temperatures [38, 39].

Table 4
Quantitative phase composition of catalyst samples after catalytic tests

Sample	Fe_3O_4	χ-Fe_5C_2	$MnCO_3$
Fe/C	56.6 mass. %	43.4 mass. %	-
Fe-Mn/C	22.1 mass. %	51.6 mass. %	26.3 mass. %

During the CO_2 hydrogenation, the formation of manganese carbonate (JCPDS 83-1763), magnetite (JCPDS 89-0688) and Hägg carbide (JCPDS 89-7272) phases occur. With crystallite size: $MnCO_3$ – 35 nm, Fe_3O_4 – 25 nm, Fe_5C_2 – 47 nm.

The quantitative composition of the studied systems was evaluated after catalytic tests by RIR method (Table 4). It can be seen that the introduction of manganese into the catalyst leads to an increase in the proportion of Hägg carbide during the Fischer-Tropsch synthesis.

Since Hägg carbide phase is responsible for the polymerization process and the growth of the hydrocarbon chain, this explains the higher yield of C_{5+} hydrocarbons compared to the unpromoted catalyst (Table 1). Moreover, in the work [31], an increase in the number of olefins and a decrease in the yield of methane are associated with the ability of magnesium to intensify the formation of iron carbide. The promoted sample contains more carbide (Table 4), which explains a decrease in the methane yield and an increased content of olefins compared to the Fe/C.

4. Conclusion

Catalytic systems based on carbonized cellulose have shown activity in the CO_2 hydrogenation reaction. It has been established that the introduction of manganese leads to the formation of a larger amount of Hägg carbide, which is responsible for the formation of C_{5+} hydrocarbons, which is confirmed by catalytic data. It is important to note that catalyst promotion significantly affected the C_{5+} liquid hydrocarbon composition: the presence of manganese led to an intensification of secondary processes with the formation of a significant amount of iso-structures in the products. With the introduction of manganese, the suppression of methane formation and an increase in the proportion of C_2-C_4 light olefins were observed.

This fact is in good agreement with the literature data where an increase in the number of olefins and a decrease in the methane yield are associated with the ability of magnesium to intensify the formation of iron carbide and reduces the hydrogenating function of the catalyst due to a decrease in H_2 adsorption and an increase in CO adsorption. An interesting feature of the composition of products obtained on catalysts based on carbonized cellulose is the distribution of C_1-C_6 alcohols.

On the Fe/C catalyst at low synthesis temperatures (240–280 °C), methanol predominated, the proportion of which decreased with increasing temperature due to more intense ethanol formation. In the products obtained on the Fe-Mn/C catalyst, the main component of the alcohol phase is ethanol. This difference indicates different routes for the C_2-C_6 alcohol formation: in the presence of the Fe/C catalyst, oxymethylene radicals are formed on the catalyst surface followed by their polycondensation, while C_{2+}OH alcohols are formed on the Fe–Mn/C catalyst by the methanol homologation reaction.

As is commonly known, in heterogeneous catalysis, the nature of the support has a significant effect on the catalytic system activity and the product composition. The materials of this article show that the carbon support obtained by hydrothermal carbonization can be successfully used as a support for carbon dioxide hydrogenation catalysts. For further improvement of catalysts of this type, these carbon materials require a comprehensive study, including using in situ methods.

Acknowledgments

This work was supported by the Russian Science Foundation under grant №17-73-30046 and performed using the equipment of the Shared Research Center “Analytical center of deep oil processing and petrochemistry of TIPS RAS”.

References

[1]. D.W. Kweku, O. Bismark, A. Maxwell, K.A. Desmond, K.B. Danso, E.A. Oti-Mensah, A.T. Quachie, B.B. Adormaa, *Journal of Scientific Research and Reports* 17 (2018) 1–9. DOI: 10.9734/JSRR/2017/39630

[2]. A. Quadrelli, SETIS magazine. Carbon Capture Utilisation and Storage 11 (2016) 8–9. https://setis.ec.europa.eu/system/files/2021-01/setis-magazine_11_ccus.pdf

[3]. F. Fischer, H. Pichler, *Brennstog-Chem.* 14 (1933) 306.

[4]. F. Fischer, Th. Bahr, H. Meusel, Brennstoff-Chem. 16 (1935) 466–469

[5]. H. Kuster, Reduction of carbon dioxide to higher hydrocarbons at atmospheric pressures

by catalysts of the iron group. *Brennstoff-Chem*, 17 (1936a), 221–228.
[6]. Z. He, M. Cui, Q. Qian, J. Zhang, H. Liu, B. Han, *Proceedings of the National Academy of Sciences* 116 (2019) 12654–12659. DOI: 10.1073/pnas.1821231116
[7]. H.M. Torres Galvis, J.H. Bitter, C.B. Khare, M. Ruitenbeek, A. Iulian Dugulan, K.P. de Jong, *Science* 335 (2012) 835–838. DOI: 10.1126/science.1215614
[8]. E. Pérez-Mayoral, V. Calvino-Casilda, E. Soriano, *Catal. Sci. Technol.* 6 (2016) 1265–1291. DOI: 10.1039/C5CY01437A
[9]. S.N. Khadzhiev, M.V. Kulikova, M.I. Ivantsov, L.M. Zemtsov, G.P. Karpacheva, D.G. Muratov, G.N. Bondarenko, N.V. Oknina, *Petrol. Chem.* 56 (2016) 522–528. DOI: 10.1134/S0965544116060049
[10]. M. Kulikova, M. Chudakova, M. Ivantsov, A. Kuz'min, A. Krylova, A.L. Maksimov, *J. Braz. Chem. Soc.* 32 (2021) 287–298. DOI: 10.21577/0103-5053.20200179
[11]. K. Krysanova, A. Krylova, V. Zaichenko, *Fuel* 256 (2019) 115929. DOI: 10.1016/j.fuel.2019.115929
[12]. M. Sevilla, A.B. Fuertes, *Carbon* 47 (2009) 2281–2289. DOI: 10.1016/j.carbon.2009.04.026
[13]. B. Hu, K. Wang, L. Wu, S.-H. Yu, M. Antonietti, M.-M. Titirici, *Adv. Mater.* 22 (2010) 813–828. DOI: 10.1002/adma.200902812
[14]. R. Li, A. Shahbazi, L. Wang, B. Zhang, C.-C. Chung, D. Dayton, Q. Yan, *Fuel* 225 (2018) 403–410. DOI: 10.1016/j.fuel.2018.03.179
[15]. J. Lv, Z. Bai, L. Yang, C. Hu, J. Zhou, *Russ. J. Electrochem.* 49 (2013) 577–582. DOI: 10.1134/S1023193512090091
[16]. P. Makowski, R. Demir Cakan, M. Antonietti, F. Goettmann, M.-M. Titirici, *Chem. Commun.* 8 (2008) 999–1001. DOI: 10.1039/b717928f
[17]. K. Sheng, S. Zhang, J. Liu, Shuang E, C. Jin, Z. Xu, X. Zhang, *J. Clean. Prod.* 237 (2019) 117831. DOI: 10.1016/j.jclepro.2019.117831
[18]. Q. Yan, C. Wan, J. Liu, J. Gao, F. Yu, J. Zhang, Zhiyong Cai, *Green Chem*. 15 (2013) 16–31. DOI: 10.1039/c3gc37107g
[19]. G. Yu, B. Sun, Y. Pei, S. Xie, S. Yan, M. Qiao, K. Fan, X. Zhang, B. Zong, *J. Am. Chem. Soc.* 132 (2010) 935–937. DOI: 10.1021/ja906370b
[20]. W. Ma, Y. Ding, J. Yang, X. Liu, L.Lin, *React. Kinet. Catal. Lett*. 84 (2005) 11–19. DOI: 10.1007/s11144-005-0185-6
[21]. M. Puccini, E. Stefanelli, A.L. Tasca, S. Vitolo, *Chem. Eng. Trans*. 67 (2018) 637–642.
[22]. K.H. Adolfsson, N. Yadav, M. Hakkarainen, *Curr. Opin. Green Sustain. Chem.* 23 (2020) 18–24. DOI: 10.1016/j.cogsc.2020.03.008
[23]. M. Martinelli, M.K. Gnanamani, S. LeViness, G. Jacobs, W.D. Shafer, *Appl. Catal. A* 608 (2020) 117740. DOI: 10.1016/j.apcata.2020.117740
[24]. W. Li, H. Wang, X. Jiang, J. Zhu, Z. Liu, X. Guo, C. Song, *RSC Advances* 8 (2018) 7651–7669. DOI: 10.1039/C7RA13546G
[25]. J. Barrault, C. Forquy, J.C. Menezo, R. Maurel, *React. Kinet. Catal. Lett.* 17 (1981) 373–378. DOI: 10.1007/BF02065849
[26]. W.-P. Ma, Y.-L. Zhao, Y.-W. Li, Y.-Y. Xu, J.-L. Zhou, *React. Kinet. Catal. Lett.* 66 (1999) 217–223. DOI: 10.1007/BF02475793
[27]. E.S. Lox, G.B. Marin, E. De Grave, P. Bussière, *Appl. Catal.* 40 (1988) 197–218. DOI: 10.1016/S0166-9834(00)80438-8
[28]. C.R. Hubbard, R.L. Snyder, *Powder Diffr.* 3 (1988) 74–77. DOI: 10.1017/S0885715600013257
[29]. Z. Tao, Y. Yang, C. Zhang, T. Li, M. Ding, H. Xiang, Y. Li, *J. Nat. Gas Chem*. 16 (2007) 278–285. DOI: 10.1016/S1003-9953(07)60060-7
[30]. M. Feyzi, F. Jafari, *J. Fuel Chem. Technol.* 40 (2012) 550–557. DOI: 10.1016/S1872-5813(12)60021-8
[31]. T. Li, Y. Yang, C. Zhang, X. An, H. Wan, Z. Tao, H. Xiang, Y. Li, F. Yi, B. Xu, *Fuel* 86 (2007) 921–928. DOI: 10.1016/j.fuel.2006.10.019
[32]. A.L. Lapidus, A.Yu. Krylova, *Ross. Khim. Zh.* 44 (2000) 43–56 (in Russ.). http://www.chem.msu.su/rus/jvho/2000-1/43.pdf
[33]. A.Y. Krylova, V.I. Kurkin, M.V. Kulikova, A.S. Lyadov, S.A. Sagitov, *Solid Fuel Chem*. 45 (2011) 281–285. DOI: 10.3103/S0361521911040069
[34]. Y.-N. Wang, W.-P. Ma, Y.-J. Lu, J. Yang, Y.-Y. Xu, H.-W. Xiang, Y.-W. Li, Y.-l. Zhao, B.-J. Zhang, *Fuel* 82 (2003) 195–213. DOI: 10.1016/S0016-2361(02)00154-0
[35]. K. Opeyemi Otun, Y. Yao, X. Liu, D. Hildebrandt, *Fuel* 296 (2021) 120689. DOI: 10.1016/j.fuel.2021.120689
[36]. G. Xu, Y. Zhu, J. Ma, H. Yan, Y. Xie, *Stud. Surf. Sci. Catal.* 112 (1997) 333–338. DOI: 10.1016/S0167-2991(97)80854-3
[37]. R. Li, L. Zhang, S. Zhu, S. Fu, X. Dong, S. Ida, L. Zhang, L. Guo, *Appl. Catal. A* 602 (2020) 117715. DOI: 10.1016/j.apcata.2020.117715
[38]. F. Lu, J. Huang, Q. Wu, Y. Zhang, *Appl. Catal. A* 621 (2021) 118213. DOI: 10.1016/j.apcata.2021.118213
[39]. W. Ben Soltan, J. Sun, W. Wang, Z. Song, X. Zhao, Y. Mao, Z. Zhang, *Sci. Total Environ.* 819 (2022) 152844. DOI: 10.1016/j.scitotenv.2021.152844